Calcium rubidium nitrate: Mode-coupling β scaling without factorization

M. Goldammer,[1,*] C. Losert,[1,†] J. Wuttke,[1,‡] W. Petry,[1] F. Terki,[2] H. Schober,[1,3] and P. Lunkenheimer[4]
[1]*Physik-Department E13, Technische Universität München, 85747 Garching, Germany*
[2]*Laboratoire de Science des Matériaux Vitreux, Université Montpellier II, 34095 Montpellier Cedex, France*
[3]*Institut Laue-Langevin, 38042 Grenoble Cedex 9, France*
[4]*Experimentalphysik V, Universität Augsburg, 86135 Augsburg, Germany*
(Received 29 January 2001; published 19 July 2001)

The fast dynamics of viscous calcium rubidium nitrate is investigated by depolarized light scattering, neutron scattering, and dielectric loss. Fast β relaxation evolves as in calcium potassium nitrate. The dynamic susceptibilities can be described by the asymptotic scaling law of mode-coupling theory with a shape parameter $\lambda = 0.79$; the temperature dependence of the amplitudes extrapolates to $T_c \simeq 378$ K. However, the frequencies of the minima of the three different spectroscopies never coincide, in conflict with the factorization prediction, indicating that the true asymptotic regime is unreachable.

DOI: 10.1103/PhysRevE.64.021303 PACS number(s): 64.70.Pf, 78.35.+c, 61.12.−q, 77.22.−d

I. INTRODUCTION

A. Motivation

Using three different spectroscopies, we have investigated the fast dynamics of glass-forming calcium rubidium nitrate. The work is motivated by unexpected differences between the high-frequency dielectric loss of calcium rubidium nitrate and that of its homologue calcium potassium nitrate [1].

The mixed salt calcium potassium nitrate (composition $[Ca(NO_3)_2]_{0.4}[KNO_3]_{0.6}$, abbreviation CKN) is one of the best studied glass formers. In particular it was among the first materials for which the relevance of mode-coupling theory (MCT) [2] was demonstrated [3–8]. In the cross-over region between microscopic dynamics and α relaxation, neutron [5] and light [6] scattering experiments could be described by the asymptotic scaling function of fast β relaxation. In this regime any dynamic susceptibility is expected to converge towards the same asymptote, which is determined by a single parameter λ. For CKN, a value $\lambda = 0.81$ was found [6].

Although the theory allows any λ between 0.5 and 1.0, experiments on many other liquids and on colloids, as well as simulations and numeric solutions of MCT for model systems yield almost always values between 0.7 and 0.8. A major exception from this has been reported for calcium rubidium nitrate (composition $[Ca(NO_3)_2]_{0.4}[RbNO_3]_{0.6}$, abbreviation CRN): Broad-band dielectric measurements suggested $\lambda = 0.91$ [1]. This is unexpected because of the close similarity between CRN and CKN [9,10], and it is interesting also because for $\lambda \to 1$ one expects logarithmic corrections to the scaling laws of MCT [11]. In order to investigate this anomaly in more detail, we have performed light and neutron scattering experiments and reanalyzed dielectric data.

B. Fast dynamics and β relaxation

To explain the focus of the present study, let us anticipate some experimental data. Figure 1 shows the dynamic susceptibility of CRN as measured by depolarized light scattering. The temperature-independent band on the high-frequency side is attributed to the microscopic dynamics: Vibration, rotation, libration. Above 3 THz the susceptibilities coin-

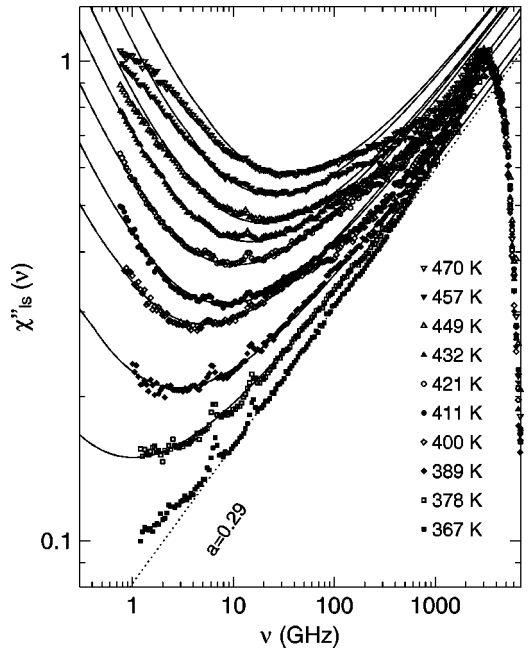

FIG. 1. Susceptibilities of CRN as measured by light scattering between 367 K (bottom) and 470 K (top). The small peaks at about 7 and 15 GHz are due to residual TA and LA Brillouin scattering. For $\nu \gtrsim 3$ THz all data fall together, as expected for harmonic vibrations. In the low-frequency, high-temperature limit the curves bend towards the α-relaxation peak. The intermediate regime of fast β relaxation can be described by the asymptotic scaling function of mode-coupling theory: the solid curves show fits (1) with a common shape parameter $\lambda = 0.79$. The dotted line shows a power-law fit to the lowest temperature from 10 to 1000 GHz. The resulting exponent of $a = 0.29$ corresponds to $\lambda = 0.78$.

*Present address: Institut für Klinische Radiologie, Klinikum Großhadern, Universität München, 81377 München, Germany.
†Present address: Siemens AG, CTMS 3, Otto-Hahn-Ring 6, 81739 München, Germany.
‡Corresponding author. Email address: jwuttke@ph.tum.de; URL: http://www.e13.physik.tu-muechen.de/Wuttke

cide for all temperatures, as expected for purely harmonic excitations. At lower frequencies, on the other hand, the dynamics is clearly anharmonic. In the low-frequency, high-temperature limit the curves bend over towards a maximum that itself remains outside the experimental frequency window. This maximum is due to structural α relaxation. It is strongly temperature dependent; its evolution towards lower temperatures and lower frequencies can be studied by many other slower spectroscopic techniques.

In the following we concentrate on the intermediate frequency range around the susceptibility minimum. In this regime, called *fast β relaxation*, one finds nontrivial contributions to the dynamic susceptibility, which can *not* be explained by a simple superposition of α relaxation and microscopic excitations. The existence of this regime has confirmed a key result of MCT.

More specific predictions have been made by analytically solving mode-coupling equations in a certain asymptotic limit: for temperatures little above a critical temperature, $T \gtrsim T_c$, and for frequencies around the susceptibility minimum, $\nu \sim \nu_\sigma$, any susceptibility is expected to converge towards the same asymptote

$$\chi''(\nu) \simeq \chi_\sigma g_\lambda(\nu/\nu_\sigma). \tag{1}$$

This is often described as a *factorization*: for instance, wave number dependent neutron scattering data $\chi''(q,\nu)$ factorize into an amplitude, which depends only on q, and a spectral distribution, which depends only on the frequency ν. The amplitudes

$$\chi_\sigma \propto |\sigma|^{1/2} \tag{2}$$

and the characteristic frequency of β relaxation

$$\nu_\sigma \propto |\sigma|^{1/2a} \tag{3}$$

are predicted to depend for all spectroscopies in the same way on the reduced temperature

$$\sigma = \frac{T_c - T}{T_c}. \tag{4}$$

The two wings of the susceptibility minimum are described by power laws

$$g_\lambda(\tilde{\nu}) \propto \begin{cases} \tilde{\nu}^{-b} & \text{for} \quad \tilde{\nu} \ll 1 \\ \tilde{\nu}^{a} & \text{for} \quad \tilde{\nu} \gg 1. \end{cases} \tag{5}$$

The fractal exponents a and b depend on the parameter λ that alone determines the full shape [12] of $g_\lambda(\tilde{\nu})$.

By now fast β relaxation has been observed in many different structural glass formers. Spectroscopic and scattering measurements on CKN, as well as on several other model systems, have been sucessfully fitted by Eqs. (1)–(3). On the other hand, more recent theoretical [13,14] and experimental [15] studies emphasize that the first-order scaling law (1) might be obscured by higher-order corrections.

In the present study we shall analyze how far an asymptotic MCT description applies to the fast dynamics of CRN. For a broader perspective on relaxation in glass-forming liquids, we refer back to reviews like [16,17] in which much wider temperature and frequency ranges are covered and several other theoretical approaches are discussed.

II. EXPERIMENTS AND RAW DATA TREATMENT

A. Samples

A mixture of calcium nitrate and rubidium nitrate, $[Ca(NO_3)_2]_{0.4}[RbNO_3]_{0.6}$, was prepared as in Ref. [1]. For the light-scattering measurements the sample material was transferred under helium atmosphere into a glass cuvette, which was sealed and mounted in a cryofurnace that can reach temperatures up to 470 K. For the neutron-scattering measurement at the Institut Laue-Langevin (ILL) the material was filled into an aluminum container [18,19] so that the sample forms a hollow cylinder of thickness 1 mm, outer radius 29 mm, and height 50 mm; the aluminum itself was 0.1 mm thick. The cell was mounted in an ILL cryo loop; a thermocouple in direct contact with the sample was used to determine the temperature.

The samples showed little tendency to crystallize, except when kept for several hours between 400 and 410 K. The glass state can be reached easily by supercooling with moderate speed ($\lesssim 5$ K/min). The glass transition temperature $T_g = 333$ K [10] of CRN is exactly the same as of CKN. The melting point of crystalline CRN has not been measured, but we suppose that it is similar to $T_m \simeq 438$ K of CKN.

B. Depolarized light scattering

Light-scattering was measured on a six-pass tandem interferometer and a two-pass grating monochromator. A near backscattering (173°) geometry with crossed polarizers (HV) was used to minimize scattering from acoustic modes. Stray light was negligible compared to the dark counts of the avalanche photodiodes. The dark count rate of about 2.5 sec^{-1} was in turn more than ten times weaker than the weakest scattering signals; nevertheless we subtracted it from all measured spectra.

For the high-frequency regime from 100 GHz to 5 THz we used a Jobin-Yvon U1000 double monochromator. The entrance and exit slits were set to 50 μm and the slits between the two monochromators to 100 μm, resulting in a full width at half maximum of 10 GHz and a stray light suppression of better than 10^{-5} at 100 GHz. To maintain this resolution over hours, days, and months the temperature of the instrument has to be stabilized carefully (± 0.05 K); therefore the monochromator is placed in an insulating box (< 0.5 W/(m^2 K)) and thermalized by forced convection: The air temperature inside the box is regulated by an electrical heater placed in front of a fan, acting against large water-cooled copper sheets.

For the low-frequency regime from 0.7 to 180 GHz we used a Sandercock-Fabry-Perot six-pass tandem interferometer, which we modified in several details as described in Ref. [15], in order to allow for stable operation and high contrast. The instrument was used in series with an interference filter of either 150 or 1000 GHz bandwidth that sup-

presses higher-order transmission leaks of the tandem interferometer [20–22] below 3% or better. The filters are placed in a specially insulated housing with active temperature stabilization. To account for any drift, the instrument function is redetermined periodically by automatic white-light scans.

In the present study we used three different free spectral ranges (188, 50, and 16.7 GHz), corresponding to mirror spacings of 0.8, 3, and 9 mm. Measured spectra were divided by the white-light transmission. Then they were converted from intensity to susceptibility

$$\chi''_{\rm ls}(\nu) = I(\nu)/n(\nu) \tag{6}$$

with the Bose factor $n(\nu) = [\exp(h\nu/k_{\rm B}T) - 1]^{-1}$; this representation is more sensitive to experimental problems. Whenever Stokes and anti-Stokes data did not fall onto each other the measurement was repeated. Finally scans taken at different spectral ranges were joined after adjusting the intensity scales by a least-square match of the overlapping data points. Additional scans at other mirror spacings confirmed the accuracy of the composite broad-band susceptibilities.

The overall intensity scale was taken from an unperturbed temperature cycle on the interferometer with a free spectral range of 188 GHz, to which all other measurements were matched. The accuracy of this procedure was confirmed in the Terahertz range, where harmonic vibrations are expected to yield a temperature-independent susceptibility: In fact our $\chi''_{\rm ls}(\nu)$ coincide within 4%.

The temperature independence of $\chi''_{\rm ls}(\nu)$ in the vibrational range was used to set the intensities of the 400 and 410 K spectra, which had to be measured separately because of the tendency to crystallize.

C. Neutron scattering

Figure 2(a) shows the static structure factor $S(q)$, measured by neutron diffraction at about room temperature, of CRN (a rapid measurement on G41 at the LLB) and of CKN (from the detailed study [23]). Except for the amplitude, no adjustments have been made. Over most of the q range, the $S(q)$ of both materials agree exceptionally well; the deviations below 1.2 Å^{-1} are most probably due to multiple scattering and other artifacts that are expected to affect mostly the low-q region. Thus we can detect no difference between the structures of CRN and CKN, although the cation diameters of Rb^+(2.94 Å) and K^+(2.66 Å) differ substantially.

Inelastic neutron scattering was measured on the time-of-flight spectrometer IN 5 at the ILL. This is a multichopper instrument that allows for free choice of the incident neutron wavelength λ_i. With increasing λ_i, the width of the instrumental resolution improves as λ_i^{-3}, on the expense of decreasing flux and decreasing wave numbers. As a compromise, we choose $\lambda_i = 8.0$ Å. This yields a resolution (full width at half maximum) of 8 GHz. Depending on temperature, we cut the inelastic data at typically 20 GHz, where the signal-to-noise ratio is of the order of 10^3.

Our choice of λ_i restricts the wave number range for elastic scattering to $q \lesssim 1.3$ Å^{-1}. Thus we do not reach the maximum of the structure factor at 1.9 Å^{-1}. Therefore we get rather low scattering intensities; fortunately, the static structure factor maximum is also inaccessible for almost all multiple-scattering events [24].

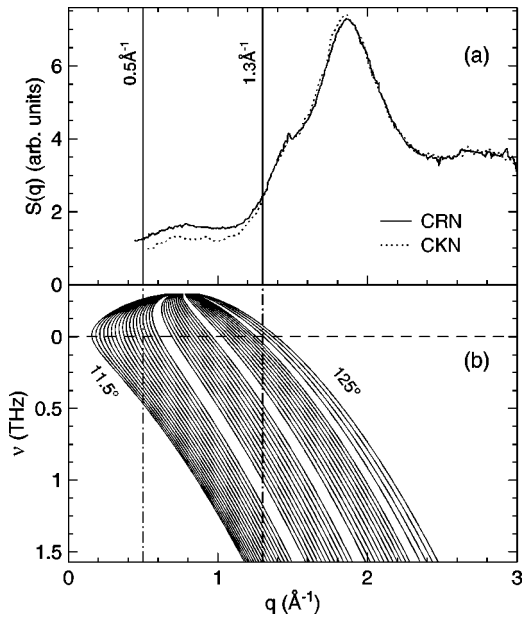

FIG. 2. (a) Static structure factor $S(q)$ of CRN (solid line, measured on G41 at the Laboratoire Léon Brillouin) and of CRN (dotted line, scanned from Ref. [23]), both obtained by neutron diffraction at about room temperature. (b) Dynamic window of our inelastic scattering experiment on the time-of-flight spectrometer IN 5 for an incident neutron wavelength $\lambda_i = 8.0$ Å. The solid curves show $q(\nu)$ for every second detector. The scattering law $S(q,\nu)$ is obtained by interpolating the constant-angle data to constant-q sections. The vertical dashed-dotted lines indicate the limits of the q range used in the data analysis.

The four chemical elements that constitute CRN are all coherent scatterers; the incoherent scattering cross sections are negligibly small. However, the mixture of elements with different coherent scattering length leads to a considerable incoherent scattering background. In the q range of our experiment the signal is mainly due to this Laue scattering.

Figure 2(b) shows the dynamic window of our measurement in the q,ν plane. The accessible $q(\nu, 2\vartheta)$ are shown for every second detector angle 2ϑ. The gaps in the plot are due to struts inside the flight chamber of the instrument.

The measured $S(\nu, 2\vartheta)$ are interpolated to constant q. Only wave numbers between 0.5 and 1.3 Å^{-1} are used in the analysis. As a last step the $S(q,\nu)$ are converted into a susceptibility $\chi''_q(\nu) = S(q,\nu)/n(\nu)$.

III. RESULTS AND ANALYSIS

A. Light-scattering results

The light-scattering data have already been presented in Sec. I B (Fig. 1). We now concentrate on the intermediate regime of fast β relaxation. At low temperatures the high-frequency wing of the susceptibility minimum follows a power law $\chi''_{\rm ls}(\nu) \propto \nu^a$. At 367 K this power law extends over two decades from 10 to 1000 GHz with $a = 0.29$. Within MCT this exponent corresponds to a shape parameter

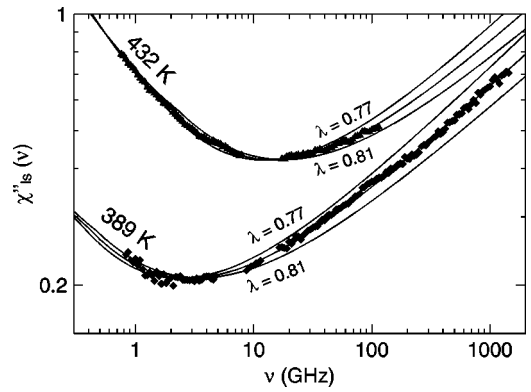

FIG. 3. A subset of the light scattering data, and mode-coupling fits with three different values of the shape parameter λ (0.77, 0.79, 0.81). At 389 K the curve with $\lambda = 0.79$ describes the data over three decades in frequency. The Brillouin peaks have been removed from the data before fitting.

$\lambda = 0.78$. This has to be compared to the dielectric measurements [1] where a similar power-law behavior has been observed over more than three decades with $a = 0.2$ for 361 K, leading to the exceptional value $\lambda = 0.91$.

Looking for the power-law asymptotes (5) is obviously not the best way of testing the applicability of MCT. The scaling prediction (1) is expected to hold best in the intermediate regime around $\nu \sim \nu_\sigma$. Therefore we use the full scaling function $\chi_\sigma g_\lambda(\nu/\nu_\sigma)$ to fit the experimental data around the minimum. Figure 3 shows such fits for two temperatures and with three different values of λ. From this comparison we obtain $\lambda = 0.79$ with an accuracy better than ± 0.01. Figure 1 contains fits with fixed $\lambda = 0.79$ for all temperatures.

From these fits we extract the amplitude χ_σ and the characteristic frequency ν_σ as functions of temperature. For constant λ, the parameters χ_σ and ν_σ are proportional to the height and the position of the susceptibility minimum. In order to test the predictions (2) and (3), Fig. 4 shows them as χ_σ^2 and ν_σ^{2a}. Linear fits to the lowest five points confirm the predictions (2), and (3) over an interval of 50 K and extrapolate consistently to a value for T_c between about 365 K and 370 K.

B. Neutron-scattering results

Compared to depolarized light scattering, neutron scattering features as an additional coordinate the wave number q. This allows for a direct test of the factorization property (1): In the asymptotic regime of fast β relaxation the susceptibility $\chi''_{\rm ns}(q,\nu)$. Such a factorization is also expected for one-phonon scattering from a harmonic system.

As described elsewhere [15,25] the h_q are determined from a least-square match of neighboring q cuts. Figure 5 shows the rescaled $\chi''_{\rm ns}(q,\nu)/h_q$; the inset shows the h_q. As in other cases the h_q do not go with q^2, which can be explained by an almost q-independent multiple-scattering background [26].

The factorization holds around the β minimum as well as for the vibrational band; only for the highest temperature the q-dependent α peak comes into the experimental window.

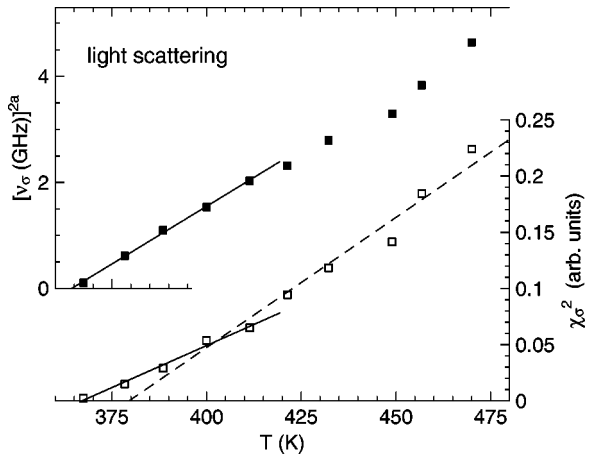

FIG. 4. Characteristic frequency (■) and amplitude (□) of the susceptibility minimum, extracted from the fits with $\lambda = 0.79$. The rectified plot of ν_σ^{2a} and χ_σ^2 *vs* T allows to check the MCT predictions (2) and (3). When the analysis is restricted to $T < 420$ K, linear fits (solid lines) give a consistent T_c between 365 and 370 K. Alternatively, a fit to χ_σ^2 for all but the two lowest temperatures yields $T_c \approx 379$ K (dashed line).

This allows us to collapse all q cuts into an average susceptibility

$$\chi''_{\rm ns}(\nu) = \langle \chi''(q,\nu)/h_q \rangle_q \tag{7}$$

with much improved statistics. Results are shown in Fig. 6.

Fits with the mode-coupling asymptote $\chi_\sigma g_\lambda(\nu/\nu_\sigma)$ allow for any value of λ between 0.7 and 0.8, but definitely not for $\lambda = 0.91$. Therefore we impose the light-scattering result λ

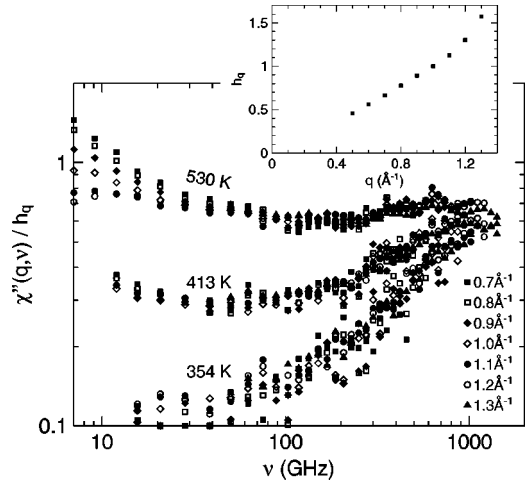

FIG. 5. Susceptibilities measured with neutron scattering. According to the factorization property of mode-coupling theory the dynamics in the fast β regime can be described by frequency-dependent part and a q-dependent factor. Using this property the susceptibilities for different q can be collapsed onto a single curve by multiplying with a temperature-independent factor h_q. At 530 K the q-dependent α peak moves into the experimental window. Apart from the α relaxation all curves can be added to improve the data quality for fits to the frequency-dependent part. The inset shows h_q as a function of q.

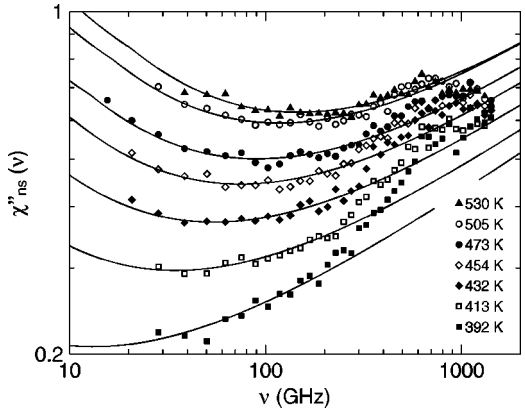

FIG. 6. Susceptibility $\chi''_{\rm ns}(\nu)=\langle\chi''(q,\nu)/h_q\rangle$ averaged over q between 0.5 and 1.3 Å^{-1} (excluding the q-dependent α relaxation in the low-frequency, high-temperature limit). Solid lines are fits to the MCT asymptote with fixed $\lambda=0.79$.

$=0.79$. For most temperatures, the fits describe the susceptibilities over one decade or more.

Towards low frequencies, the fit range is restricted by the instrumental resolution, except for the highest temperatures where α relaxation is resolved (Fig. 5). On the high-frequency side, the fit range extends up to about 200 GHz. At higher frequencies neutron-scattering data rise *above* the fit, whereas light-scattering data fall *below* the theoretical curves. This gives an upper limit for the frequency range of the asymptotic regime of fast β relaxation.

A rectified plot of the β-relaxation parameters is shown in Fig. 7. The amplitude χ_σ follows the power law (2) over 140 K, a much wider temperature interval than in light scattering. The straight line fitted to χ^2_σ extrapolates to $T_c \simeq 380$ K. On the other hand, the frequency ν_σ does not obey (3). At high temperatures, the ν_σ^{2a} seem to lie on a line that extrapolates to an unphysical T_c far below T_g. For lower temperatures, the data possibly bend over towards the true asymptote, which, however, is not reached in our experiment. At this point we should note that the ν_σ are much more sensitive to noise and to remnants of the instrumental resolution than the χ_σ.

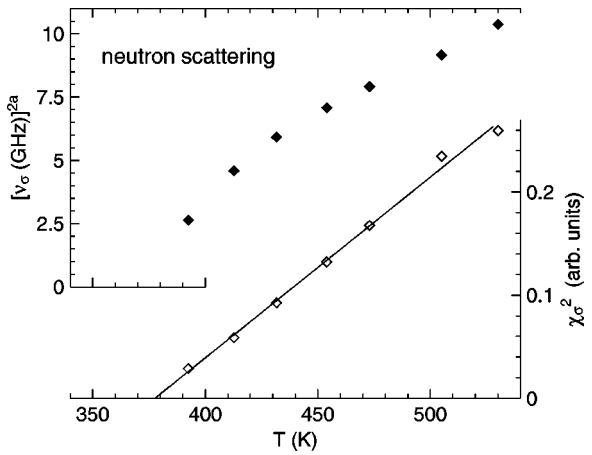

FIG. 7. A rectified plot of the β-relaxation parameters determined by neutron scattering does not extrapolate to a consistent value for T_c. While χ^2_σ suggest an extrapolation to $T_c \simeq 380$ K, the ν_σ^{2a} do not reach the asymptote (3).

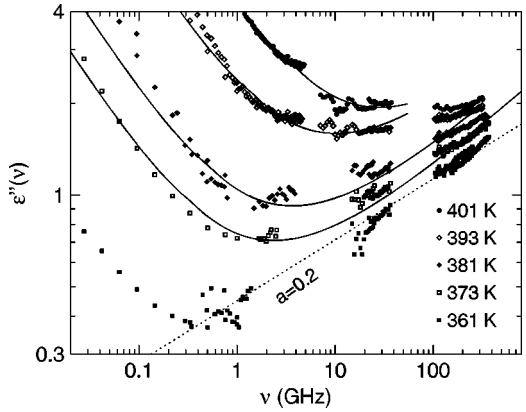

FIG. 8. Dielectric loss between 361 K (bottom) and 401 K (top). Solid lines show the mode-coupling asymptote with an imposed parameter $\lambda=0.79$. These fits work well around the susceptibility minimum, but they do not match the exceptionally small slope of the high-frequency wing. The dotted line shows the power-law asymptote corresponding to $\lambda=0.91$ used in the original publication [1].

C. Reanalyzing dielectric data

Dielectric loss has been measured in CRN over more than 11 decades in frequency, from 1 mHz to 380 GHz [1]. Here we concentrate on the fast β relaxation. The most remarkable feature of this regime is the extremely slow increase of $\epsilon''(\nu)$ on the high-frequency side of the minimum. For three decades in frequency (40 MHz−40 GHz) $\epsilon''(\nu)$ follows a power law with an exponent $a=0.2$. As anticipated above, this implies $\lambda=0.91$. Using this value, the dielectric data could be fitted with the scaling function $\epsilon_\sigma g_\lambda(\nu/\nu_\sigma)$ over a wide range, extending from about the minimum up to the highest measured frequencies.

As we have seen above, $\lambda=0.91$ is not compatible with the light- and neutron-scattering results. Furthermore we have seen that the asymptotic regime does not extend above some 100 GHz. Therefore we now reanalyze the dielectric data with an imposed value $\lambda=0.79$, concentrating on lower frequencies. The resulting fits are shown in Fig. 8. As expected, the fits do not match the high-frequency wings (the data fall below the fit function, as in light scattering); on the other hand, the fits now cover much of the $\nu<\nu_\sigma$ wing.

The two fit parameters are shown in Fig. 9. The ϵ^2_σ suggest $T_c \simeq 377$ K. Within their experimental uncertainty, the ν_σ^{2a} seem compatible with such an extrapolation; their determination suffers however from the hitherto unavoidable frequency gaps in the dielectric broad-band measurements.

IV. COMPARISON OF THE THREE SPECTROSCOPIES

For each of the three spectroscopic techniques employed in this study, we found a fast β relaxation. For each of the three data sets, we verified the asymptotic validity of the

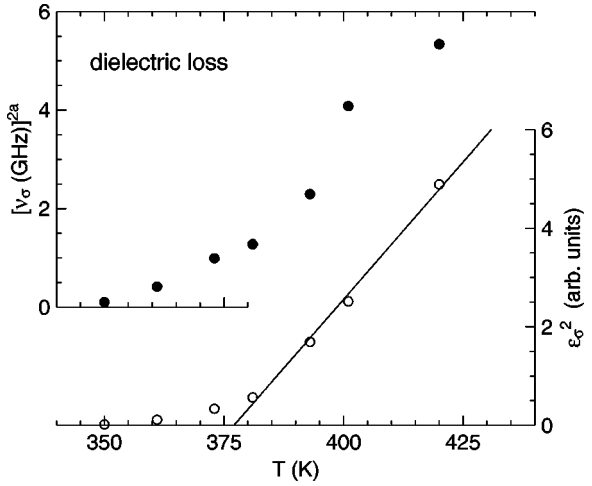

FIG. 9. As in Figs. 4 and 7, this plot shows frequency and amplitude of fast β relaxation, extracted from fits with $\lambda = 0.79$ and rectified according to the MCT predictions.

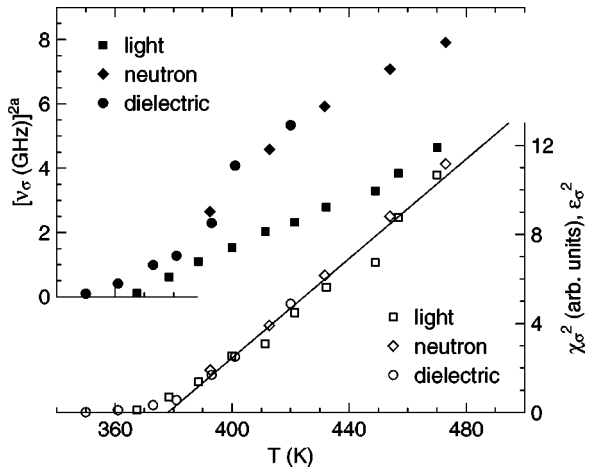

FIG. 10. All rectifications combined in one figure. While the amplitudes χ_σ^2 extrapolate to a consistent $T_c \simeq 378$ K for all methods, the position ν_σ differ considerably.

scaling function (1), and we found the temperature-dependent parameters at least in partial accord with the power laws (2) and (3).

The next question is whether the fits to the individual data sets are consistent with each other. From the factorization property of fast β relaxation we expect that all susceptibilities converge towards the *same* frequency and temperature dependence. Anticipating this prediction, we have already imposed *one* value $\lambda = 0.79$ to the analysis of all three data sets. Our fits confirm that all data can indeed be described by the same scaling function $\chi_\sigma g_\lambda(\nu/\nu_\sigma)$.

Additionally we expect a consistent temperature dependence of all amplitude χ_σ and frequencies ν_σ. *A fortiori*, power-law fits to these parameters must extrapolate toward a unique value of T_c. In Sec. III linear fits to the χ_σ^2 gave

T_c	From method	Range
$\simeq 367$ K	Light scattering	378–412 K
$\simeq 378$ K	Neutron scattering	392–530 K
$\simeq 377$ K	Dielectric loss	381–420 K.

The spread of these T_c's is definitely larger than the uncertainty of the experimental temperature scale. In order to reach a consistent interpretation of the three data sets, we replot in Fig. 10 all MCT parameters on a common temperature scale. The amplitudes are scaled by an arbitrary factor. In this representation all χ_σ^2 above about 390 K appear compatible with a common power law (2). This suggests a reinterpretation of the light-scattering data. Shifting the fit range to higher temperatures we find indeed

T_c	From method	Range
$\simeq 379$ K	Light scattering	389–470 K

as shown by the dashed line in Fig. 4. Thus the amplitudes χ_σ can be given a consistent MCT interpretation with a common $T_c \simeq 378 \pm 2$ K.

The same is not true for the frequencies ν_σ. In light scattering we had found a consistent asymptotic temperature dependence of ν_σ and χ_σ. This accord is however lost after shifting the fit range to higher temperatures: A free fit to the ν_σ does not help to obtain a T_c above 370 K. In neutron scattering the ν_σ do not reach the power-law regime at all. Only in dielectric loss the ν_σ are possibly compatible with $T_c \simeq 378$ K.

Furthermore, within the asymptotic regime the ν_σ are expected to agree in absolute value. The comparison in Fig. 10 shows that this is not the case for any temperature. This violation of the MCT factorization prediction is also confirmed by the direct comparison of measured susceptibilities

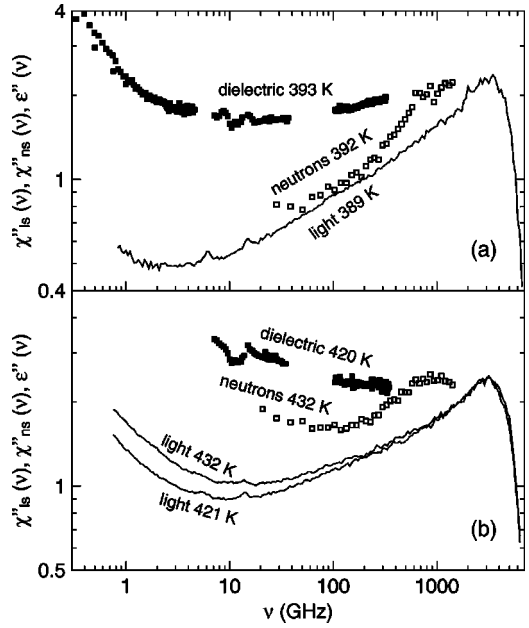

FIG. 11. A direct comparison of the three methods on arbitrary susceptibility scale: (a) all three spectroscopies at about 390 K; (b) a pairwise comparison of neutron and light scattering at 432 K, and of dielectric loss and light scattering at 420 K. The minimum positions are grossly different even if each curve for itself seemed describable by the mode-coupling asymptote.

in Fig. 11: The positions of the minima differ by up to a factor 10. While each data set for itself seemed to be in good accord with the scaling predictions of MCT it now turns out that most if not all data are outside the true asymptotic regime.

V. COMPARISON WITH OTHER GLASS FORMERS

A. CRN and CKN

We undertook this work with the intention of comparing CRN to the well-studied model liquid CKN. In planning and performing the scattering experiments we took full advantage of the experience gained in previous investigations, and we intentionally concentrated on the temperature and frequency window of fast β relaxation. Therefore it is not surprising that by now our CRN data are more accurate and more complete than what has been published many years ago on CKN.

CKN was the material in which Cummins and coworkers first discovered the self-similarity of depolarized light-scattering spectra [27]. Subsequent broad-band measurements were successfully described by the scaling laws of MCT, leading to $\lambda = 0.81 \pm 0.05$ and $T_c = 378 \pm 5$ K [6]. Later the light-scattering susceptibilities were also fitted across T_c with extended MCT [7]. Unfortunately, these studies, as any other at that time, had been undertaken with an unsufficient bandpass in the tandem interferometer [20–22]. Higher-order leaks cause distortions of the spectral line shapes that are most harmful at low temperatures. Above T_c, all qualitative observations will remain valid, but as we have shown in the case of propylene carbonate [15] the parameter λ might change by as much as 0.06.

CKN was also the material in which neutron-scattering experiments by Mezei and co-workers first showed the relevance of MCT. Elastic scans gave the first evidence for the onset of fast β relaxation on approaching T_c, estimated at about 368 K [4]. Later Mezei emphasized the uncertainty of this determination [28]. Combined backscattering and time-of-flight measurements revealed the crossover between the asymptotic power laws $S(q,\nu) \propto \nu^{-1-b}$ and ν^{-1+a} [5]; a free fit of a gave $\lambda \simeq 0.80$ whereas a consistent set of a and b suggested $\lambda \simeq 0.89$. More recent neutron-scattering experiments concentrated on α relaxation [29], on the static structure factor [23,30], and on the microscopic dynamics above 100 GHz [24,30,31]; a state-of-the-art determination of λ and T_c for CKN is presently missing.

In contrast, dielectric loss in CKN has been measured recently [1] and with the same accuracy as in CRN. MCT fits to the CKN data gave $\lambda \simeq 0.76$ and $T_c \simeq 375$ K.

In this situation, it would be worthwhile to remeasure the dynamic susceptibility of CKN at selected temperatures above T_c by light and neutron scattering. Such measurements would allow to determine more precise values of λ and T_c, to crosscheck the β relaxation parameters obtained by different spectroscopies, and then to compare in more detail the overall behavior of CKN to that of CRN.

On the basis of the available data we can conclude that as soon as we restrict our analysis to frequencies below about 100 GHz there is no significant difference in the fast dynamics of CKN and CRN. The uncertainty in the determination of λ, especially for CKN, is presently much larger than any difference between CKN and CRN. Since both materials have the same calorimetric glass transition temperature, it is not unreasonable to compare also the T_c's on absolute scale; the value 378 K for CRN agrees perfectly well with the best available estimates for CKN.

B. CRN and organic glass formers

Similar studies of fast β relaxation have already been undertaken in a number of organic glass formers. Light and neutron scattering around the susceptibility minimum have been compared in glycerol [32], salol [33], toluene [34], and trimethylheptane [35]. In propylene carbonate [15] the scattering experiments have also been compared to dielectric and time-dependent optical measurements.

Most of these studies show the same trend as the present CRN data: Individual data sets seem in good accord with the scaling predictions of MCT, but the positions of the susceptibility minima do not coincide. A major exception is provided by glycerol where the factorization property seems to hold although the individual data sets do not reach the MCT asymptote [32].

In CRN and in toluene, the susceptibility minimum lies at lower frequencies for light scattering than for neutron scattering, whereas in salol, trimethylheptane and propylene carbonate the opposite is observed. On this basis it is presently impossible to give any microscopic explanation [35].

We do understand why fast β relaxation appears in the dielectric loss data only within a rather small temperature range (up to about 40 K above T_c, whereas neutron-scattering data show a β minimum up to at least $T_c + 150$ K): As explained for the case of propylene-carbonate [15] this is an immediate consequence of the scaling behavior of α relaxation. Since the α peak (relative to the susceptibility in the phonon range) is much stronger in dielectric loss than in the scattering experiments, it begins at relatively low temperatures to hide the β minimum.

VI. CONCLUSION

With each sample we investigate it becomes clearer that fast β relaxation is a constitutive property of viscous liquids. If we want to understand the macroscopic behavior of glass-forming materials, we will have to understand the full evolution of fast dynamics from phonons towards α relaxation, which inevitably involves β relaxation.

In CRN, as in many other systems [36], dynamic susceptibilities in the β regime show at least partial acccord with the first-order scaling predictions of MCT. Fits with Eqs. (1)–(3) provide a valuable parametrization of the experimental data, and they help to uncover the universal behavior of different materials. Nevertheless, such fits are potentially misleading. Even the best fits do not guarantee that the true asymptotic regime is reached: any additional measurement can disprove the factorization.

Yet a failure of the asymptotic factorization is not a failure of MCT. The decisive physical approximations which must

be experimentally tested are made in deriving, not in solving the mode-coupling equations. Even for a simple model that obeys MCT by construction the asymptotic β regime is only reached at very low frequencies and for temperatures very close to T_c [13,14]. These conditions are never reached in experiments on realistic structural glass formers: even if the dynamic range and the signal-to-noise ratio of future spectrometers allowed such measurements, the β relaxation of idealized MCT would be covered by hopping processes.

On this background it might even surprise that remnants of the scaling behavior (1)–(3) are actually observed in molecular systems. This is possibly explained by analytic expansions beyond the first-order scaling laws [13] that suggest that susceptibilities are severely distorted in the preasymptotic regime while the amplitudes χ_σ still evolve in good accord with the power law (2).

For a more specific analysis we have to await a theory that takes into account the molecular structure of our liquid. In the recent years considerable progress has been made in extending MCT to molecular systems [37–39]. A theory of CKN or CRN seems not out of reach. However, until then we can compare experimental results only to asymptotic scaling laws or to numeric solutions of schematic mode-coupling models.

In propylene carbonate it has been explicitly shown [40] that the different experimental susceptibilities can be described by simultaneous fits with a few-parameter mode-coupling model. We have no doubt that similar fits would also work in CRN. Considering however that we found no qualitative difference between CRN and CKN, we suggest that any additional experimental and theoretical effort be invested in the generally recognized model system CKN.

ACKNOWLEDGMENTS

We thank A. Maiazza (TU Darmstadt) for preparing the sample material used in all three spectroscopies, and G. André (LLB Saclay) for measuring the structure factor of CRN. We acknowledge financial aid by the Bundesministerium für Bildung, Wissenschaft, Forschung und Technologie through Verbundprojekte 03PE4TUM9 and 03LO5AU28 and through Contract No. 13N6917, by the Deutsche Forschungsgemeinschaft under Grant No. LO264/8–1.

[1] P. Lunkenheimer, A. Pimenov and A. Loidl, Phys. Rev. Lett. **78**, 2995 (1997).
[2] W. Götze, in *Liquids, Freezing and the Glass Transition*, Proceeding of the Les Houches Summer School, Session LI, edited by J. P. Hansen, D. Levesque, and D. Zinn-Justin (North Holland, Amsterdam, 1991).
[3] F. Mezei, W. Knaak, and B. Farago, Phys. Rev. Lett. **58**, 571 (1987).
[4] F. Mezei, W. Knaak, and B. Farago, Phys. Scr., T **19**, 363 (1987).
[5] W. Knaak, F. Mezei and B. Farago, Europhys. Lett. **7**, 527 (1988).
[6] G. Li *et al.*, Phys. Rev. A **45**, 3867 (1992).
[7] H.Z. Cummins *et al.*, Phys. Rev. E **47**, 4223 (1993).
[8] Y. Yang and K.A. Nelson, J. Chem. Phys. **104**, 5429 (1996).
[9] C.A. Angell, J. Phys. Chem. **70**, 2793 (1966).
[10] A. Pimenov *et al.*, J. Non-Cryst. Solids **220**, 93 (1997).
[11] W. Götze and L. Sjögren, J. Phys.: Condens. Matter **1**, 4203 (1989).
[12] W. Götze, J. Phys.: Condens. Matter **2**, 8485 (1990).
[13] T. Franosch *et al.*, Phys. Rev. E **55**, 7153 (1997).
[14] M. Fuchs, W. Götze, and M.R. Mayr, Phys. Rev. E **58**, 3384 (1998).
[15] J. Wuttke *et al.*, Phys. Rev. E **61**, 2730 (2000).
[16] H.Z. Cummins *et al.*, Z. Phys. B: Condens. Matter **103**, 501 (1997).
[17] P. Lunkenheimer, U. Schneider, R. Brand and A. Loidl, Contemp. Phys. **41**, 15 (2000).
[18] J. Wuttke, Physica B **266**, 112 (1999).
[19] J. Wuttke, Physica B **292**, 194 (2000).
[20] N.V. Surovtsev *et al.*, Phys. Rev. B **58**, 14 888 (1998).
[21] J. Gapinski *et al.*, J. Chem. Phys. **110**, 2312 (1999).
[22] H.C. Barshilia, G. Li, G.Q. Shen, and H.Z. Cummins, Phys. Rev. E **59**, 5625 (1999).
[23] E. Kartini *et al.*, Can. J. Phys. **73**, 748 (1995).
[24] M. Russina *et al.*, Phys. Rev. Lett. **84**, 3630 (2000).
[25] J. Wuttke *et al.*, Z. Phys. B: Condens. Matter **91**, 357 (1993).
[26] J. Wuttke, Phys. Rev. E **62**, 6531 (2000).
[27] N.J. Tao, G. Li, and H.Z. Cummins, Phys. Rev. Lett. **66**, 1334 (1991).
[28] F. Mezei, Ber. Bunsenges. Phys. Chem. **95**, 1118 (1991).
[29] E. Kartini and F. Mezei, Physica B **213**, 486 (1995).
[30] E. Kartini *et al.*, Phys. Rev. B **54**, 6292 (1996).
[31] F. Mezei and M. Russina, J. Phys.: Condens. Matter **11**, A341 (1999).
[32] J. Wuttke *et al.*, Phys. Rev. Lett. **72**, 3052 (1994).
[33] J. Toulouse, R. Pick, and C. Dreyfus, in *Disordered Material and Interfaces*, edited by H. E. Stanley et al., Mater. Res. Soc. Symp. Proc. No. 407 (Materials Research Society, Pittsburgh, 1996), p. 161.
[34] J. Wuttke *et al.*, Eur. Phys. J. B **1**, 169 (1998).
[35] G.Q. Shen *et al.*, Phys. Rev. E **62**, 783 (2000).
[36] Tests of mode-coupling theory have been reviewed recently by W. Götze, J. Phys.: Condens. Matter **11**, A1 (1999).
[37] L. Fabbian *et al.*, Phys. Rev. E **62**, 2388 (2000).
[38] W. Götze, A.P. Singh, and T. Voigtmann, Phys. Rev. E **61**, 6934 (2000).
[39] C. Theis *et al.*, Phys. Rev. E **62**, 1856 (2000).
[40] W. Götze and T. Voigtmann, Phys. Rev. E **61**, 4133 (2000).